The Size Dependence of Phytoplankton Growth Rates: A Trade-Off between Nutrient Uptake and Metabolism

Ben A. Ward,[1,*] Emilio Marañón,[2] Boris Sauterey,[3,4] Jonathan Rault,[4] and David Claessen[4]

1. School of Geographical Sciences, University of Bristol, University Road, Bristol BS8 1SS, United Kingdom; 2. Departamento de Ecología y Biología Animal, Universidade de Vigo, 36310 Vigo, Spain; 3. Department of Biology, University of Kentucky, Lexington, Kentucky; 4. Ecole Normale Supérieure, Paris Sciences et Lettres Research University, Institut de Biologie de l'Ecole Normale Supérieure, Centre National de la Recherche Scientifique Unité Mixte de Recherche 8197, Institut National de la Santé et de la Recherche Médicale U1024, 46 Rue d'Ulm, F-75005 Paris, France

Submitted August 12, 2016; Accepted October 12, 2016; Electronically published December 12, 2016

Online enhancements: appendixes.

abstract: Rates of metabolism and population growth are often assumed to decrease universally with increasing organism size. Recent observations have shown, however, that maximum population growth rates among phytoplankton smaller than ~6 μm in diameter tend to increase with organism size. Here we bring together observations and theory to demonstrate that the observed change in slope is attributable to a trade-off between nutrient uptake and the potential rate of internal metabolism. Specifically, we apply an established model of phytoplankton growth to explore a trade-off between the ability of cells to replenish their internal quota (which increases with size) and their ability to synthesize new biomass (which decreases with size). Contrary to the metabolic theory of ecology, these results demonstrate that rates of resource acquisition (rather than metabolism) provide the primary physiological constraint on the growth rates of some of the smallest and most numerically abundant photosynthetic organisms on Earth.

Keywords: metabolic theory, resource uptake, allometry, power law, unimodal, monomodal.

Introduction

The maximum growth rate of biological populations (μ_{max}) is an important determinant of community composition and ecosystem function. It constrains both the relative success of species during exponential growth, and the outcome of resource competition when mortality rates are high. The metabolic theory of ecology proposes that the maximum growth rate is controlled by the metabolic rate (Brown et al. 2004), itself limited by fundamental constraints on the distribution of resources within organisms (West et al. 1997; Banavar et al. 2002). These are argued to be such that temperature-corrected rates of metabolism and population growth should vary with cell volume, V, as a simple power-law function of the form $\mu_{max} = aV^b$ (i.e., a linear relationship between $\log(\mu_{max})$ and $\log(V)$). The intercept, a, gives the maximum growth rate at $V = 1$ μm^3, while the exponent, b, describes the slope of $\log(\mu_{max})$ as a function of $\log(V)$, with a predicted value of -0.25 (West et al. 1997). This prediction for the population growth rate has been confirmed across a broad range of organisms, spanning more than 12 orders of magnitude in body mass (Fenchel 1973; Blueweiss et al. 1978; Peters 1983; Savage et al. 2004). Mounting empirical evidence suggests, however, that maximum growth rates deviate from the predicted monotonic power-law relationship among unicellular organisms smaller than approximately 10 μm in diameter (DeLong et al. 2010; Kempes et al. 2012). Among the phytoplankton in particular, a number of studies have observed that maximum population growth rates show a unimodal size dependence, with a peak somewhere in the 2–20-μm-diameter size range (Raven 1994; Bec et al. 2008; Chen and Liu 2010; Finkel et al. 2010; Marañón et al. 2013). An example of this unimodal size dependence is shown in figure 1.

It is important that we understand these deviations from the metabolic theory of ecology, because microbial organisms are central to the function of marine communities and the Earth system. Marine plankton are responsible for approximately half of global net primary production (Field et al. 1998) and form the foundation of all pelagic ecosystems. In this capacity, they support essential nutrition to more than half the world's population via fisheries (Hollowed et al. 2013) and play a critical role in maintaining the Earth's climate at a habitable level (Hain et al. 2014). Organism size is an important aspect of these large-scale ecological and biogeochemical processes (Falkowski and Oliver 2007), and a number of theoretical explanations have been put forward to explain

* Corresponding author; e-mail: b.a.ward@bristol.ac.uk.

ORCIDs: Ward, http://orcid.org/0000-0003-1290-8270; Sauterey, http://orcid.org/0000-0001-6164-756X; Claessen, http://orcid.org/0000-0001-7354-1316.

Am. Nat. 2017. Vol. 189, pp. 000–000.
DOI: 10.1086/689992

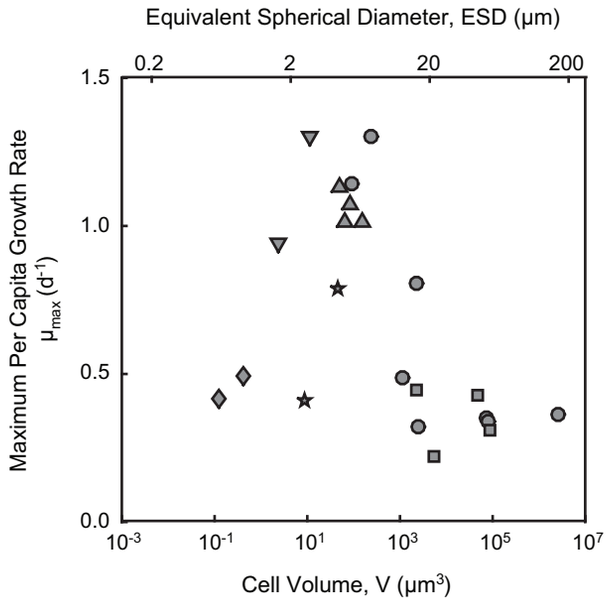

Figure 1: Experimentally observed size dependence of the maximum per capita population growth rate (μ_{max}) in experiments reported by Marañón et al. (2013). Note that these data represent the net phytoplankton growth rate, as calculated in appendix A (available online). Diamond, cyanobacteria; down-pointing triangle, chlorophyte; star, other; up-pointing triangle, coccolithophore; circle, diatom; square, dinoflagellate.

the unimodal pattern seen in figure 1. These have focused variously on nutrient storage capacity (Verdy et al. 2009), resource distribution within the cell (Wirtz 2011), mortality (Kempes et al. 2012), exudation (Kriest and Oschlies 2007), and thermal adaptation (Sal et al. 2015). Empirical support for these theories has, however, typically come from meta-analysis of compiled data rather than from direct experimental tests. It has therefore been difficult to assess the validity of these competing ideas.

In this article, we use observations derived from a single set of experiments (using the same laboratory protocols; Marañón et al. 2013) to explore the pattern shown in figure 1. We will apply these observations within a formal mathematical framework (Burmaster 1979) to show that the observed unimodal size dependence of μ_{max} is attributable to a size-dependent trade-off between metabolism and nutrient uptake (Marañón et al. 2013; Marañón 2015). In this way, we will present a simple, mechanistic explanation of why phytoplankton population growth rates deviate from the metabolic theory of ecology at very small size.

Phytoplankton Growth Model

We wish to assess the idea that the size dependence of the maximum population growth rate is dictated by the balance of nutrient uptake and metabolism (Marañón et al. 2013; Marañón 2015). We therefore apply a phytoplankton growth model that considers both these processes (Caperon 1968; Droop 1968). The model assumes that the per capita population growth rate (μ) is set as a hyperbolic function of the cellular nutrient quota (Q). Following Burmaster (1979) and consistent with the measurements of Marañón et al. (2013), we define the cell quota in terms of nitrogen biomass per cell. Net population growth requires a quota in excess of the basal cellular nutrient requirement (Q_{min}) and increases with increasing Q toward a theoretical maximum metabolic rate, μ_∞. This is effectively the maximum possible rate of cell division assuming an infinite (and unobtainable) internal nutrient reserve (Caperon 1968; Droop 1968):

$$\mu = \mu_\infty \left(1 - \frac{Q_{min}}{Q}\right). \tag{1}$$

The cellular nutrient quota itself is supplied by nutrient uptake (ρ) and is diluted as cells divide (μQ). The rate of change in Q is therefore given by

$$\frac{dQ}{dt} = \rho - \mu Q. \tag{2}$$

Nutrient uptake is typically assumed to be a saturating (Michaelis-Menten-like) function of environmental nutrient availability. In this study, we are concerned with only periods of nutrient-saturated growth, and so we assume that nutrient uptake is equal to the maximum saturated rate ($\rho = \rho_{max}$). For the sake of simplicity, we ignore the possibility that nutrient uptake is downregulated as the cell quota approaches a maximum capacity. While this mechanism can be important in terms of regulating the size of the nutrient quota when the maximum uptake rate is large relative to the growth rate (Grover 1991), we show in appendix B (apps. A, B are available online) that accounting for the maximum quota has a negligible impact on the size dependence of the maximum per capita growth rate (μ_{max}).

We assume that nutrient uptake is balanced by cell division during nutrient-saturated exponential growth, such that equation (2) can be rewritten as $\rho_{max} = \mu_{max} Q$. This equality can then be substituted into equation (1) to obtain an expression for the maximum phytoplankton growth rate as a function of the three physiological trait parameters (Burmaster 1979):

$$\mu_{max} = \frac{\mu_\infty \rho_{max}}{\mu_\infty Q_{min} + \rho_{max}}. \tag{3}$$

This equation demonstrates that the maximum phytoplankton growth rate is a composite trait that emerges through the interaction of more fundamental traits relating to biomass-specific nutrient uptake and metabolism. The influence of each fundamental trait on the maximum growth rate is best understood by considering equation (3) in two key limits. In

the first limit, the maximum rate of nutrient uptake (ρ_{max}) is assumed to be much slower than the maximum potential rate of cellular metabolism ($\mu_\infty Q_{min}$), and equation (3) can be approximated by

$$\mu_{max} \approx \frac{\rho_{max}}{Q_{min}} \text{ if } \rho_{max} \ll \mu_\infty Q_{min}. \quad (4)$$

In this limit, the maximum growth rate is effectively set by the maximum rate at which the basal cellular nutrient requirement (Q_{min}) can be replenished by nutrient uptake (ρ_{max}). Alternatively, the second limit assumes that ρ_{max} is much faster than $\mu_\infty Q_{min}$, and equation (3) can be approximated by

$$\mu_{max} \approx \mu_\infty \text{ if } \rho_{max} \gg \mu_\infty Q_{min}. \quad (5)$$

In this limit, the maximum growth rate is set by the maximum metabolic rate (μ_∞). We will use these fundamental limits to illustrate how the two key rates change in importance as a function of phytoplankton size.

Observations

Marañón et al. (2013) measured the population growth of 22 species of phytoplankton, spanning a size range of 0.6–168 μm equivalent spherical diameter (ESD; 0.1–2.5 × 10^6 μm^3 by volume). The growth of each species was assessed individually in batch cultures, with population size recorded in terms of cell abundance, particulate organic nitrogen, and particulate organic carbon. Marañón et al. (2013) estimated the maximum phytoplankton growth rate (μ_{max}) as the linear rate of change in the natural logarithm of cell abundance at the peak of the exponential phase. Here, μ_{max} was estimated by fitting a time-dependent sigmoidal function to the natural logarithm of cell abundance (see app. A). The advantage of this approach is that it uses all the cell abundance data collected throughout each culture experiment and is free from subjective decisions as to when the exponential phase occurs (Zwietering et al. 1990). The use of cell abundance data is consistent with the units of the model, but these data were found to be unreliable in four cultures (*Melosira numoloides*, *Thalassiosira rotula*, *Coscinodiscus radiatus*, and *Coscinodiscus wailesii*). For these species, μ_{max} was instead calculated by fitting the sigmoidal function to the natural logarithm of particulate organic carbon (app. A).

Cellular nitrogen quotas (Q) were determined throughout the batch culture experiments by dividing the concentration of particulate organic nitrogen by the cell abundance. The minimum quota (Q_{min}) for each species was determined simply as the smallest cellular quota recorded throughout the duration of each experiment. It should be noted that these values may significantly overestimate the size of the minimum quota in some cases. This is because cells can often metabolize stored nutrients during short periods of nutrient scarcity (Litchman et al. 2009), and the transient nature of the batch culture experiments makes it difficult to assess whether this reserve has been fully exhausted (see "Discussion").

The maximum nitrogen uptake rate (ρ_{max}) was determined for nutrient-starved cells as the maximum per capita rate at which nitrogen was removed from the culture medium. This was determined over short experimental periods of ≤45 min in order to capture any short periods of rapid nutrient uptake.

The maximum potential metabolic rate (μ_∞) is not directly observable. Instead, we can rearrange equation (3) to estimate μ_∞ from the directly observed values of μ_{max}, ρ_{max}, and Q_{min}:

$$\mu_\infty = \frac{\mu_{max}\,\rho_{max}/Q_{min}}{\rho_{max}/Q_{min} - \mu_{max}}. \quad (6)$$

Note that this estimate can become increasingly sensitive to small measurement errors when $\mu_{max} \approx \rho_{max}/Q_{min}$ (i.e., eq. [4]). We show later that this issue is most apparent among smaller cells, for which μ_∞ has very little influence on μ_{max}. For three of the smallest species, observed values of μ_{max} actually exceeded ρ_{max}/Q_{min}, and a meaningful solution to equation (6) could not be obtained. All data used to constrain the model are reported in appendix A.

Parameterization

Figure 2 indicates that the three fundamental model parameters (ρ_{max}, Q_{min}, and μ_∞) all show a clear linear relationship with cell volume, V, when plotted on logarithmic axes. They can, therefore, be well described by power-law functions of the form $p = aV^b$ (where p is the parameter value). The initial values (and associated 95% confidence intervals) for coefficients a and b were found for each parameter by reduced major axis regression. The coefficients yielded at this first stage are hereafter referred to as the initial estimates.

The initial estimates were subsequently adjusted within their 95% confidence limits in order to maximize the fit of equation (3) to observations of μ_{max}. This was done using lsqcurvefit, a nonlinear least squares curve-fitting package in Matlab 2015a. The coefficient values after this second stage are hereafter referred to as the adjusted estimates.

Results

Power-law functions describing the size dependence of the three model parameters are shown in figure 2. Dashed lines represent the initial estimates, while solid lines represent the adjusted estimates that maximize the fit of equation (3) to observed values of μ_{max}. The initial and adjusted estimates (and associated 95% confidence intervals) for coefficients a and b are given in table 1. It should be noted that two of

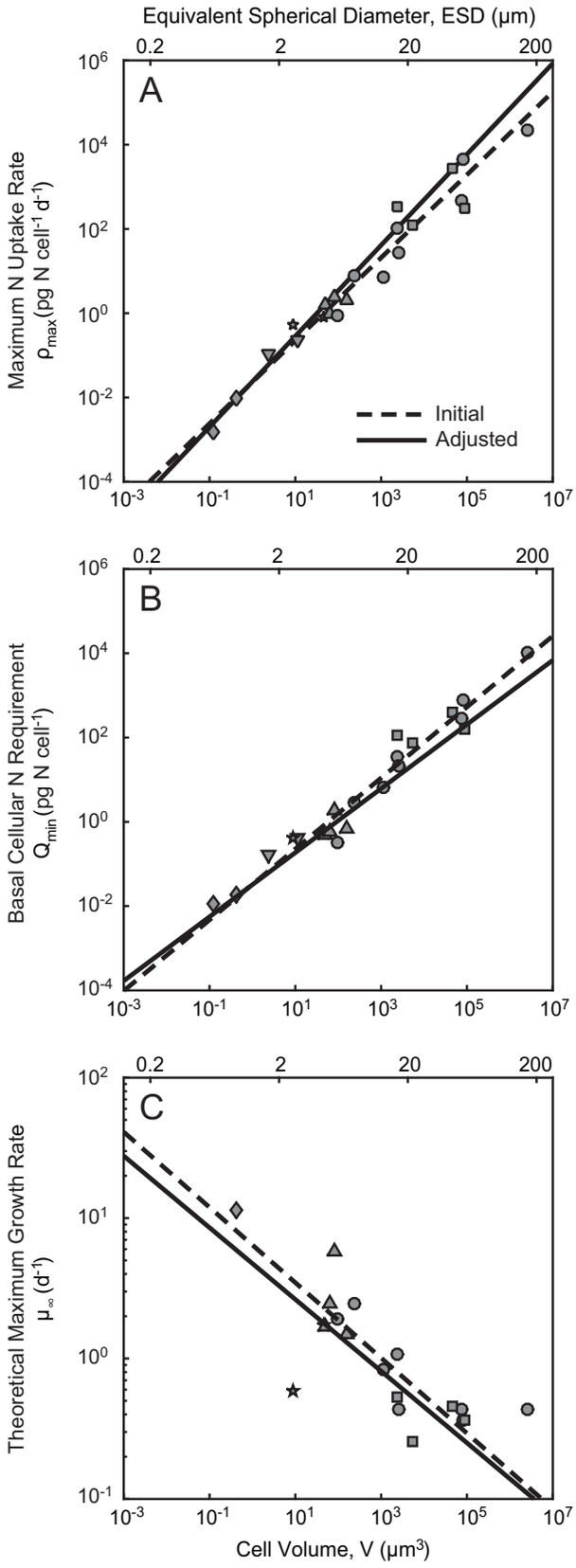

the six coefficients took values at the extremes of their initial confidence limits. This issue is addressed in the discussion.

Figure 3 shows the initial and adjusted fit of equation (3) to observed values of μ_{max}. The initial fit captures the unimodal shape of the data but underestimates the negative slope of the curve in the sub ~6 μm ESD size range. This issue was resolved by the adjustment step, which allowed the model to more accurately reproduce the observed μ_{max} data, improving the coefficient of determination (R^2) from 0.56 to 0.64.

Limiting Factors

The theoretical model predicts that the maximum growth rate (μ_{max}) is set either by the maximum nutrient uptake rate relative to the basal nutrient requirement (ρ_{max}/Q_{min}; eq. [4]) or by the maximum metabolic rate (μ_∞; eq. [5]). We assess this possibility here using output from the adjusted model. Figure 4*A* shows the model size dependences of μ_{max} and ρ_{max}/Q_{min}, alongside observations of ρ_{max}/Q_{min}. Both the model and data suggest that the maximum population growth rate among smaller cells is set by the maximum nutrient uptake rate relative to the basal nutrient requirement as an increasing function of organism size. Among cells larger than ~6 μm ESD, however, μ_{max} falls increasingly below ρ_{max}/Q_{min}. This suggests that some other factor limits the maximum growth rate of the larger organisms. Figure 4*B* shows the modeled size dependences of μ_{max} and μ_∞ alongside the indirect empirical estimates of μ_∞. Here the model and data suggest that with increasing size, the declining maximum metabolic rate takes over as the primary constraint on the maximum population growth rate.

Discussion

The metabolic theory of ecology predicts that population growth rates should increase universally with decreasing organism size (Brown et al. 2004). However, this prediction is refuted among the smallest and most abundant organisms. Observations have shown that maximum growth rates among prokaryotes and some very small unicellular eukaryotes actually decrease with decreasing organism size (Kempes et al. 2012; Marañón et al. 2013). This deviation

Figure 2: Size dependence of the model parameters: maximum nutrient uptake rate, ρ_{max} (*A*); minimum nutrient quota, Q_{min} (*B*); and growth rate at infinite quota, μ_∞ (*C*). Note that μ_∞ could not be estimated for three smaller taxa (see "Observations"). In each plot, dashed lines show the initial relationships yielded when fitting the power-law functions directly to the plotted data. Solid lines show the adjusted estimates derived by fitting equation (3) to the observed values of μ_{max} (see table 1 and "Parameterization"). Diamond, cyanobacteria; down-pointing triangle, chlorophyte; star, other; up-pointing triangle, coccolithophore; circle, diatom; square, dinoflagellate.

Table 1: Initial and adjusted power-law coefficients for each parameter shown in figure 2, with 95% confidence limits for the initial estimates

		Initial estimates		95% confidence limits		Adjusted estimates	
Parameter aV^b	Units	a	b	a	b	a	b
ρ_{max}	pg N cell^{-1} day^{-1}	.023	.98	.013–.042	.89–1.10	.024	1.10
Q_{min}	pg N cell^{-1}	.033	.84	.020–.054	.76–.93	.032	.76
μ_∞	day^{-1}	6.40	−.27	3.6–12.0	−.35 to −.18	4.7	−.26

Note: In each case, a gives the value of the parameter at $V = 1\ \mu m^3$, while b describes the slope of the log-transformed parameters as functions of $\log(V)$. Note that the adjusted exponents (b) of ρ_{max} and Q_{min} took values at the extremes of their initial confidence limits.

from the metabolic theory of ecology appears to apply universally to both autotrophic and heterotrophic organisms (DeLong et al. 2010) but was examined here using an important group of photosynthetic unicellular organisms.

Among this group of marine phytoplankton, Marañón et al. (2013) showed that maximum growth rates tend to decline on either side of a peak at ~6 μm ESD. We have used a simple and well-established model of phytoplankton growth (Droop 1968; Burmaster 1979) to show that this pattern is attributable to a size-dependent conflict between fundamental physiological traits. The maximum nutrient uptake rate relative to the basal nutrient requirement (ρ_{max}/Q_{min}) scales positively with size. In contrast, the theoretical maximum metabolic rate (μ_∞) scales negatively with size. At ~6 μm ESD, the two rates converge, such that μ_{max} among smaller cells is set by the rate at which the internal quota can be replenished by nutrient uptake, while μ_{max} among larger cells is limited by the rate at which the internal nutrient quota can be converted into new biomass.

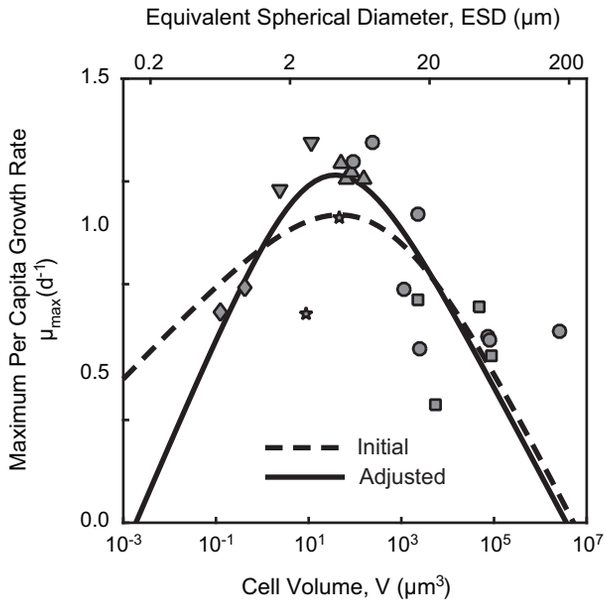

Figure 3: Initial and adjusted estimates of μ_{max} given by equation (3). Symbols show the same observational data as in figure 1. Diamond, cyanobacteria; down-pointing triangle, chlorophyte; star, other; up-pointing triangle, coccolithophore; circle, diatom; square, dinoflagellate.

The observed fundamental traits that underpin μ_{max} conform to simple allometric power laws (table 1; fig. 2). These can be compared with theoretical predictions. In conjunction with the model, the directly observed traits imply a size-dependent slope for μ_∞ of -0.27 ± 0.09, not significantly different from the value of -0.25 that is predicted by the metabolic theory of ecology. When the model parameters were further adjusted to observations of μ_{max}, the slope for μ_∞ moved even closer to theory, taking a value of -0.26. The size dependence of μ_∞, which can be thought of as representing the maximum potential metabolic rate, is therefore consistent with the predictions of the metabolic theory of ecology.

At the other end of the size spectrum, the positive relationship between the maximum growth rate and cell size is not consistent with the metabolic theory of ecology. We have shown that the increasing trend is driven by a size-dependent increase in the maximum nutrient uptake rate relative to the minimum nutrient quota (ρ_{max}/Q_{min}), with a combined exponent of 0.34. It should be noted that this high value is dependent on adjusted exponents for ρ_{max} and Q_{min} that are at the upper and lower extremes, respectively, of their initial confidence intervals (table 1). This raises some concern about the validity of the model, but it is likely that both adjusted exponents are compensating for a probable bias in the initial estimate for the exponent of Q_{min}. This bias occurs because transient batch culture experiments tend to overestimate the size of the minimum quota among larger cells with increased capacity for nutrient storage. A more accurate way to evaluate Q_{min} is to grow cultures in chemostats with very low nutrient supply rates. Such experiments were performed for *Synechococcus* (~0.9 μm), *Emiliania huxleyi* (~7 μm), and *Skeletonema costatum* (~8 μm) under conditions that were otherwise equivalent to the Marañón et al. (2013) batch culture experiments (E. Marañón, unpublished data). It was found that the original experiments overestimated Q_{min}, more strongly in the larger cells (by 11%, 22%, and 55%, respec-

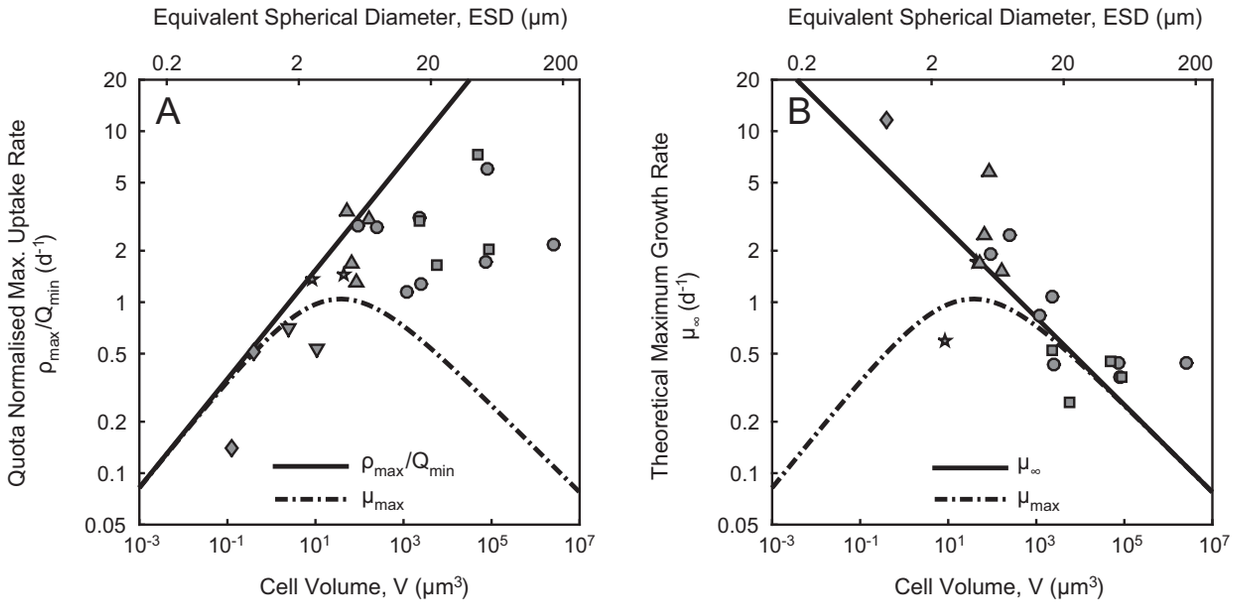

Figure 4: Factors constraining μ_{max}. Dot-and-dash lines show the adjusted model estimate of μ_{max} given by equation (3). In *A*, the solid line indicates the adjusted model size dependence of ρ_{max}/Q_{min}. In *B*, the solid line indicates the adjusted model size dependence of μ_{∞}. Note that while the symbols in *A* represent direct observations, the symbols in *B* represent model-derived estimates for μ_{∞}, as given by equation (6). Diamond, cyanobacteria; down-pointing triangle, chlorophyte; star, other; up-pointing triangle, coccolithophore; circle, diatom; square, dinoflagellate.

tively). As a consequence of this bias, the initial estimate for the slope of Q_{min} is likely too high, causing the adjustment step to choose values at the bottom of the initial range for Q_{min} and at the top of the initial range for ρ_{max}. We examined the plausibility of this argument by repeating the analysis, excluding all Q_{min} data for cells larger than 6 μm. In this case, the initial range for the exponent of Q_{min} was considerably lower, and the adjusted exponents of Q_{min} and ρ_{max} were well within the initial confidence intervals (and within ~1% the initial best estimates; see table B1; tables A1, B1 are available online). Perhaps more importantly, the omission of the potentially biased Q_{min} data had almost no effect on the adjusted fit of equation (3) to the μ_{max} data (fig. B1*B*; figs. A1, B1 are available online), and the adjusted slope of ρ_{max}/Q_{min} was almost unchanged at 0.32. This suggests that the positive slope of ρ_{max}/Q_{min} is robust to the likely overestimation of Q_{min} among the larger cells.

Leaving these issues aside, the positive slope for μ_{max} among the smallest phytoplankton is dependent on Q_{min} increasing less rapidly with cell volume than ρ_{max}. Regardless of the data used, the slope of Q_{min} was found to have an exponent of <1, approximately in line with previous estimates of 0.77 (Litchman et al. 2007) and 0.88 (Edwards et al. 2012). These low values are not surprising because of the increasing proportion of essential and nonscalable nitrogenous components (such as the genome and cellular membranes) in smaller cells (Raven 1994). On the other hand, we found the exponent of ρ_{max} to be either approximately equal to or greater than 1. These high values were not expected, because previous meta-analyses and theoretical arguments (based on consideration of the surface area to volume ratio) have suggested a slope of 2/3 (or slightly higher when accounting for nonspherical shapes among larger cells; Litchman et al. 2007; Edwards et al. 2012). The data used in this study—derived from a single set of experiments performed under identical laboratory conditions—indicate that ρ_{max} scales as an approximately isometric (i.e., linear) function of cell volume (Marañón et al. 2013). This appears to be related to a size-dependent increase in the maximum rate of nutrient uptake per unit of cellular surface area (Marañón et al. 2013), although the underlying cause of this increased uptake capacity remains an open question. Further experimental work will therefore be required to explore the isometric scaling of ρ_{max}, which appears essential to the observed unimodal size dependence of μ_{max}.

In conclusion, we have used laboratory measurements and an established model of phytoplankton growth to show that the unimodal size dependence of the maximum growth rate is attributable to a size-dependent trade-off between resource acquisition and the maximum metabolic rate. Contrary to the metabolic theory of ecology, the rate at which the internal nutrient quota can be replenished by nutrient uptake appears to be the primary constraint on the maximum growth rates of the smallest and most abundant pho-

tosynthetic organisms in the ocean. Our analysis provides a new mechanistic framework to understand an important physiological trade-off and should inspire further experimental work that will help to clarify the overarching rules that govern the size-dependent physiology of phytoplankton and other microbial organisms.

Acknowledgments

We would like to thank S. Hall for his patient efforts during the review process. His detailed and constructive comments have helped to greatly improve the clarity and accessibility of the finished article. We would also like to thank two anonymous reviewers, whose comments led to an improved overall analysis. B.A.W. gratefully acknowledges support from the Past Links in the Evolution of Ocean's Global Environment and Ecology (PALEOGENiE) project (ERC-2013-CoG-617313) and thanks the Marine Systems Modelling group at the National Oceanography Centre, Southampton. E.M. was supported by the Spanish National Plan for Scientific Research and Innovation through research grants PERSEO (CTM2007-28925- E/MAR) and TERRIFIC (CTM2014-53582-R). D.C., B.S., and J.R. received financial support from the French National Research Agency through project ANR-10-BLAN-1709 PHYTBACK.

Literature Cited

Banavar, J. R., J. Damuth, A. Maritan, and A. Rinaldo. 2002. Supply-demand balance and metabolic scaling. Proceedings of the National Academy of Sciences of the USA 99:10506–10509.

Bec, B., Y. Collos, A. Vaquer, D. Mouillot, and P. Souchu. 2008. Growth rate peaks at intermediate cell size in marine photosynthetic picoeukaryotes. Limnology and Oceanography 53:863–867.

Blueweiss, L., H. Fox, V. Kudzma, D. Nakashima, R. Peters, and S. Sams. 1978. Relationships between body size and some life history parameters. Oecologia (Berlin) 37:257–272.

Brown, J. H., J. F. Gillooly, A. P. Allen, V. M. Savage, and G. B. West. 2004. Toward a metabolic theory of ecology. Ecology 85:1771–1789.

Burmaster, D. E. 1979. The continuous culture of phytoplankton: mathematical equivalence among three steady-state models. American Naturalist 113:123–134.

Caperon, J. 1968. Growth response of *Isochrysis galbana* to nitrate variation at limiting concentrations. Ecology 49:886–872.

Chen, B., and H. Liu. 2010. Relationships between phytoplankton growth and cell size in surface oceans: interactive effects of temperature, nutrients, and grazing. Limnology and Oceanography 55: 965–972.

DeLong, J. P., J. G. Okie, M. E. Moses, R. Sibly, and J. H. Brown. 2010. Shifts in metabolic scaling, production, and efficiency across major evolutionary transitions of life. Proceedings of the National Academy of Sciences of the USA 107:12941–12945.

Droop, M. R. 1968. Vitamin B12 and marine ecology. IV. The kinetics of uptake, growth and inhibition in *Monochrysis lutheri*. Journal of the Marine Biological Association of the United Kingdom 48:689–733.

Edwards, K. F., M. K. Thomas, C. A. Klausmeier, and E. Litchman. 2012. Allometric scaling and taxonomic variation in nutrient utilization traits and maximum growth rate of phytoplankton. Limnology and Oceanography 57:554–566.

Falkowski, P. G., and M. J. Oliver. 2007. Mix and match: how climate selects phytoplankton. Nature Reviews Microbiology 5:813–819.

Fenchel, T. 1973. Intrinsic rate of natural increase: the relationship with body size. Oecologia (Berlin) 14:317–326.

Field, C. B., M. J. Behrenfeld, J. T. Randerson, and P. G. Falkowski. 1998. Primary production of the biosphere: integrating terrestrial and oceanic components. Science 281:237–240.

Finkel, Z. V., J. Beardall, K. J. Flynn, A. Quigg, T. A. V. Rees, and J. A. Raven. 2010. Phytoplankton in a changing world: cell size and elemental stoichiometry. Journal of Plankton Research 32:119–137.

Grover, J. P. 1991. Resource competition in a variable environment: phytoplankton growing according to the variable-internal-stores model. American Naturalist 138:811–835.

Hain, M. P., D. M. Sigman, and G. H. Haug. 2014. The biological pump in the past. Pages 485–517 *in* H. Holland and K. Turekian, eds. Treatise on geochemistry. Vol. 8. The oceans and marine geochemistry. 2nd ed. Elsevier, Amsterdam.

Hollowed, A. B., M. Barange, R. J. Beamish, K. Brander, K. Cochrane, K. Drinkwater, M. G. G. Foreman, et al. 2013. Projected impacts of climate change on marine fish and fisheries. ICES Journal of Marine Science 5:1023–1037.

Kempes, C. P., S. Dutkiewicz, and M. J. Follows. 2012. Growth, metabolic partitioning, and the size of microorganisms. Proceedings of the National Academy of Sciences of the USA 109:495500.

Kriest, I., and A. Oschlies. 2007. Modelling the effect of cell-size-dependent nutrient uptake and exudation on phytoplankton size spectra. Deep-Sea Research I 54:1593–1618.

Litchman, E., C. A. Klausmeier, O. M. Schofield, and P. G. Falkowski. 2007. The role of functional traits and trade-offs in structuring phytoplankton communities: scaling from cellular to ecosystem level. Ecology Letters 10:1170–1181.

Litchman, E., C. A. Klausmeier, and K. Yoshiyama. 2009. Contrasting size evolution in marine and freshwater diatoms. Proceedings of the National Academy of Sciences of the USA 106:26652670.

Marañón, E. 2015. Cell size as a key determinant of phytoplankton metabolism and community structure. Annual Review of Marine Science 7:241–264.

Marañón, E., P. Cermeño, D. C. López-Sandoval, T. Rodríguez-Ramos, C. Sobrino, M. Huete-Ortega, J. M. Blanco, and J. Rodríguez. 2013. Unimodal size scaling of phytoplankton growth and the size dependence of nutrient uptake and use. Ecology Letters 16:371–379.

Peters, R. H. 1983. The ecological implications of body size. Cambridge University Press, Cambridge.

Raven, J. A. 1994. Why are there no picoplanktonic O_2 evolvers with volumes less than 10^{-19} m^3? Journal of Plankton Research 16:565–580.

Sal, S., L. Alonso-Sáez, J. Bueno, F. C. García, and Á. López-Urrutia. 2015. Thermal adaptation, phylogeny, and the unimodal size scaling of marine phytoplankton growth. Limnology and Oceanography 60:1212–1221.

Savage, V. M., J. F. Gillooly, J. H. Brown, G. B. West, and E. L. Charnov. 2004. Effects of body size and temperature on population growth. American Naturalist 163:429–441.

Verdy, A., M. J. Follows, and G. Flierl. 2009. Optimal phytoplankton cell size in an allometric model. Marine Ecology Progress Series 379: 1–12.

West, G. B., J. H. Brown, and B. J. Enquist. 1997. A general model for the origin of allometric scaling laws in biology. Science 276:122–126.

Wirtz, K. W. 2011. Non-uniform scaling in phytoplankton growth rate due to intracellular light and CO_2 decline. Journal of Plankton Research 33:1325–1341.

Zwietering, M. H., I. Jongenburger, F. M. Rombouts, and K. van 't Riet. 1990. Modelling of the bacterial growth curve. Applied and Environmental Microbiology 56:1875–1881.

Associate Editor: Spencer R. Hall
Editor: Alice A. Winn

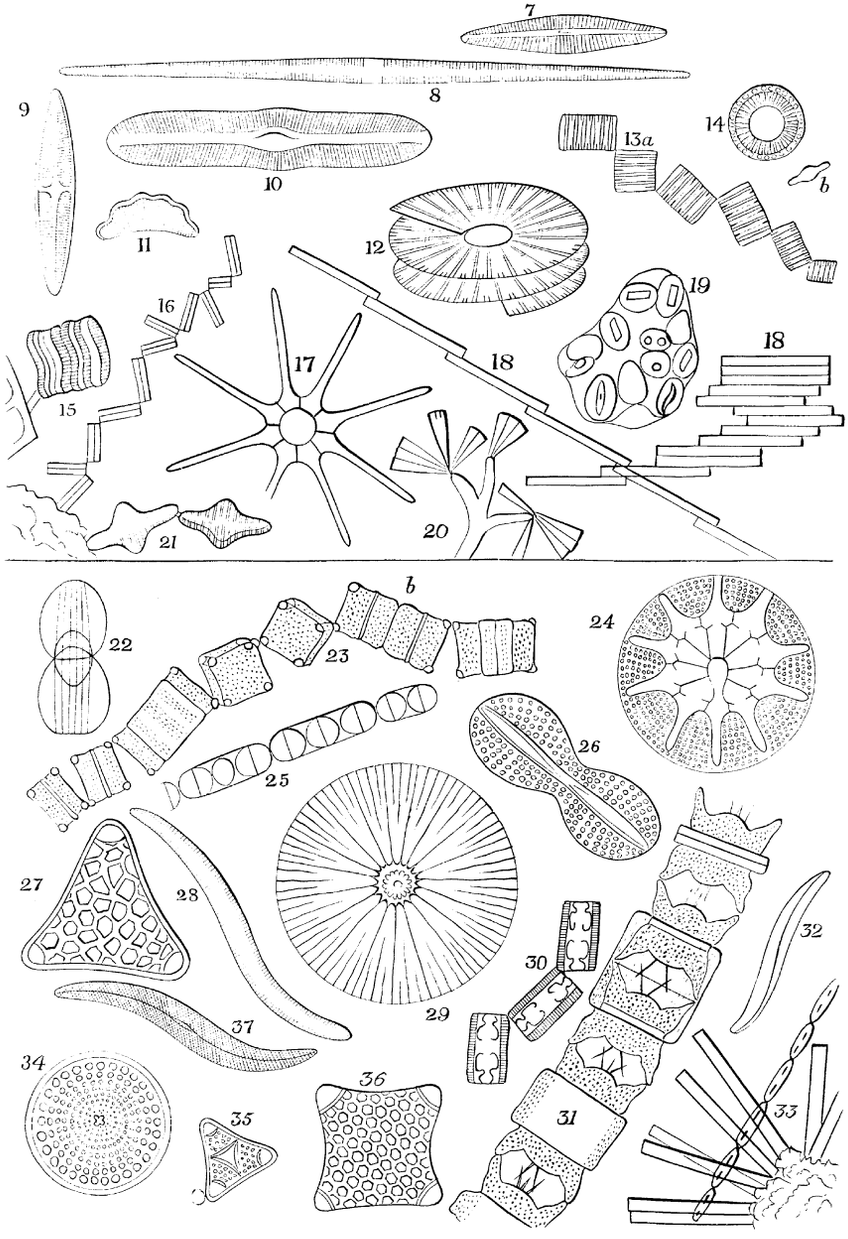

"Diatoms, —*Fresh-water*. 7, Navicula; 8, Nitschia; 9, Stauroneis; 10, Pinnularia; 11, Eunotia triodon; 12, Meridion vernale; 13, Tabellaria flocculosa, —*a*, front view, *b*, side view; 14, Cyclotella Kützingiana, —*b*, side view; 15, Acnanthes; 16, Diatoma flocculosum; 17, Asterionella; 18, Bacillaria paradoxa; 19, Mastogloia; 20, Licmophora; 21, Odontidium. . . . Diatoms, —*Marine Forms*. 22, Amphiprora; 23, Amphitetras, forming a zigzag chain, —*a*, a frustule about to divide into two, *b*, two frustules newly formed but not yet separated; 24, Asteromphalus, a beautiful deep-sea form, taken from below 2,000 fathoms in the sea of Kamschatka; 25, Podosira; 26, Navicula didyma; 27, Triceratium; 28, Nitschia; 29, Arachnoidiscus; 30, Grammatophora; 31, Biddulphia, —*a*, two frustules, still enclosed by the "connecting membranes," *b*, "connecting membrane," widening previous to self-division; 32, Pleurosigma; 33, Synedra; 34, Cosclinodiscus; 35, Triceratium; 36, Amphitetras." From "Desmids and Diatoms" by L. W. Bailey (*The American Naturalist* 1867, 1:505–517).

 DOI: 10.1086/689992

Appendix A from B. A. Ward et al., "The Size Dependence of Phytoplankton Growth Rates: A Trade-Off between Nutrient Uptake and Metabolism" (Am. Nat., vol. 189, no. 2, p. 000)

Population Growth Rates

We explain here the methods used to estimate the maximum growth rates used in the main text. We also present the source data used in all calculations. Note that the time-dependent cellular abundance, $X(t)$, is abbreviated as X.

The per capita growth rate, μ, of a phytoplankton population with cellular abundance, X, is defined as

$$\mu = \frac{1}{X}\frac{\mathrm{d}X}{\mathrm{d}t}. \tag{A1}$$

From this, we can rewrite the right-hand side as the derivative of the integral with respect to t, which gives

$$\mu = \frac{\mathrm{d}}{\mathrm{d}t}\ln(X). \tag{A2}$$

This states that the per capita growth rate is equal to the rate of change of the log-transformed abundance. The maximum rate of change under nutrient-replete growth therefore defines the maximum growth rate, μ_{max}. In figure A1, we plot the time evolution of $\ln(X/X_0)$ throughout the batch culture experiments of Marañón et al. (2013). In terms of gradient, this is equivalent to equation (A2) but has the advantage of masking the ~15 orders of magnitude variation in abundance between the smallest and largest species. For species with poor-quality data for cell abundance (*Melosira numoloides*, *Thalassiosira rotula*, *Coscinodiscus radiatus*, and *Coscinodiscus wailesii*), μ_{max} was instead estimated according to the rate of change in log-transformed particulate organic carbon (POC; $\ln(\mathrm{POC}/\mathrm{POC}_0)$).

The phytoplankton cultures described by Marañón et al. (2013) mostly follow the classic sigmoidal pattern of microbial growth. The experiments begin in the lag phase, with an initially low or zero growth rate that accelerates toward a maximum value during the exponential phase. Toward the end of the experiments, the growth rate returns to 0 as nutrients are exhausted. A widely applied approach to estimating the maximum value of μ_{max} is to perform a linear regression on a subset of the data during the exponential phase (e.g., Marañón et al. 2013). This approach necessitates discarding a large fraction of the experimental data and can be sensitive both to errors in the small number of data and to the choice of data points to represent the exponential phase. A preferable approach is to use a model to directly estimate μ_{max} as a function of all data in the experiments (Zwietering et al. 1990).

Here we chose to model the time evolution of $y = \ln(X)$ using a sigmoidal function that can represent all three phases of growth in terms of three biologically meaningful parameters (Zwietering et al. 1990).

$$y = \frac{A}{1 + \exp[(4\mu_{max}/A)(\lambda - t) + 2]}. \tag{A3}$$

This form has the advantage that the maximum per capita growth rate during the exponential phase, μ_{max}, is explicitly represented in the model. Specifically, μ_{max} describes the maximum gradient of the sigmoidal curve at its inflection point. The model also includes two other biologically meaningful parameters. The lag time, λ, is defined as time at which the tangent to the curve at its inflection point is equal to 0 (see fig. A1). Finally, the maximum population density is given by e^A. Equation (A3) was fitted to the log-transformed observations using the nonlinear least-squares solver lsqcurvefit in Matlab 2015a.

Table A1: Observed traits of the 22 phytoplankton species (Marañón et al. 2013), appearing in order of increasing cell size

Taxon	Group	Volume (μm^3)	ESD (μm)	ρ_{max} (pg N cell^{-1} day^{-1})	Q_{min} (pg N cell^{-1})	ρ_{max}/Q_{min} (day^{-1})	μ_{max} (day^{-1})	μ_∞ (day^{-1})
Prochlorococcus sp.	Cyanobacteria	1.20×10^{-1}	6.12×10^{-1}	1.53×10^{-3}	1.10×10^{-2}	1.39×10^{-1}	4.15×10^{-1}	...
Synechococcus sp.	Cyanobacteria	4.10×10^{-1}	9.22×10^{-1}	9.74×10^{-3}	1.90×10^{-2}	5.13×10^{-1}	4.91×10^{-1}	1.15×10^{1}
Ostreococcus tauri	Chlorophyte	2.40	1.66	1.13×10^{-1}	1.60×10^{-1}	7.08×10^{-1}	9.42×10^{-1}	...
Nannochloropsis gaditana	Other	8.60	2.54	5.40×10^{-1}	4.00×10^{-1}	1.35	4.10×10^{-1}	5.89×10^{-1}
Micromonas pusilla	Chlorophyte	1.10×10^{1}	2.76	2.32×10^{-1}	4.30×10^{-1}	5.40×10^{-1}	1.30	...
Pavlova lutheri	Other	4.50×10^{1}	4.41	7.94×10^{-1}	5.50×10^{-1}	1.44	7.87×10^{-1}	1.73
Calcidiscus leptoporus	Coccolithophore	5.10×10^{1}	4.60	1.63	4.80×10^{-1}	3.40	1.13	1.69
Isochrysis galbana	Coccolithophore	6.40×10^{1}	4.96	9.86×10^{-1}	5.80×10^{-1}	1.70	1.01	2.49
Gephyrocapsa oceanica	Coccolithophore	8.20×10^{1}	5.39	2.36	1.80	1.31	1.07	5.78
Phaeodactylum tricornutum	Diatom	9.30×10^{1}	5.62	8.71×10^{-1}	3.10×10^{-1}	2.81	1.14	1.92
Emiliania huxleyi	Coccolithophore	1.58×10^{2}	6.71	2.09	6.80×10^{-1}	3.07	1.01	1.51
Skeletonema costatum	Diatom	2.42×10^{2}	7.73	8.04	2.90	2.77	1.30	2.45
Thalassiosira weisflogii	Diatom	1.16×10^{3}	1.30×10^{1}	7.42	6.40	1.16	4.85×10^{-1}	8.34×10^{-1}
Melosira numoloides[a]	Diatom	2.28×10^{3}	1.63×10^{1}	1.08×10^{2}	3.50×10^{1}	3.10	8.04×10^{-1}	1.09
Protoceratium reticulatum	Dinoflagellate	2.38×10^{3}	1.66×10^{1}	3.48×10^{2}	1.16×10^{2}	3.00	4.48×10^{-1}	5.27×10^{-1}
Thalassiosira rotula[a]	Diatom	2.60×10^{3}	1.71×10^{1}	2.69×10^{1}	2.10×10^{1}	1.28	3.24×10^{-1}	4.34×10^{-1}
Alexandrium minutum	Dinoflagellate	5.58×10^{3}	2.20×10^{1}	1.21×10^{2}	7.30×10^{1}	1.65	2.23×10^{-1}	2.58×10^{-1}
Akashiwo sanguinea	Dinoflagellate	4.73×10^{4}	4.49×10^{1}	2.83×10^{3}	3.92×10^{2}	7.22	4.28×10^{-1}	4.55×10^{-1}
Dytilum brightwelli	Diatom	7.58×10^{4}	5.25×10^{1}	4.78×10^{2}	2.75×10^{2}	1.74	3.50×10^{-1}	4.38×10^{-1}
Coscinodiscus radiatus[a]	Diatom	8.20×10^{4}	5.39×10^{1}	4.70×10^{3}	7.73×10^{2}	6.09	3.41×10^{-1}	3.61×10^{-1}
Alexandrium tamarense	Dinoflagellate	8.88×10^{4}	5.54×10^{1}	3.14×10^{2}	1.55×10^{2}	2.03	3.08×10^{-1}	3.63×10^{-1}
Coscinodiscus wailesii[a]	Diatom	2.50×10^{6}	1.68×10^{2}	2.27×10^{4}	1.05×10^{4}	2.16	3.64×10^{-1}	4.38×10^{-1}

Note: Values of μ_∞ were not directly observed but were estimated from observed values of ρ_{max}, Q_{min}, and μ_{max} in equation (6) (meaningful values of μ_∞ could not be calculated for three species with measured values of μ_{max} in excess of ρ_{max}/Q_{min}). ESD, equivalent spherical diameter.

[a] Species whose growth rates were estimated from particulate organic carbon rather than abundance data.

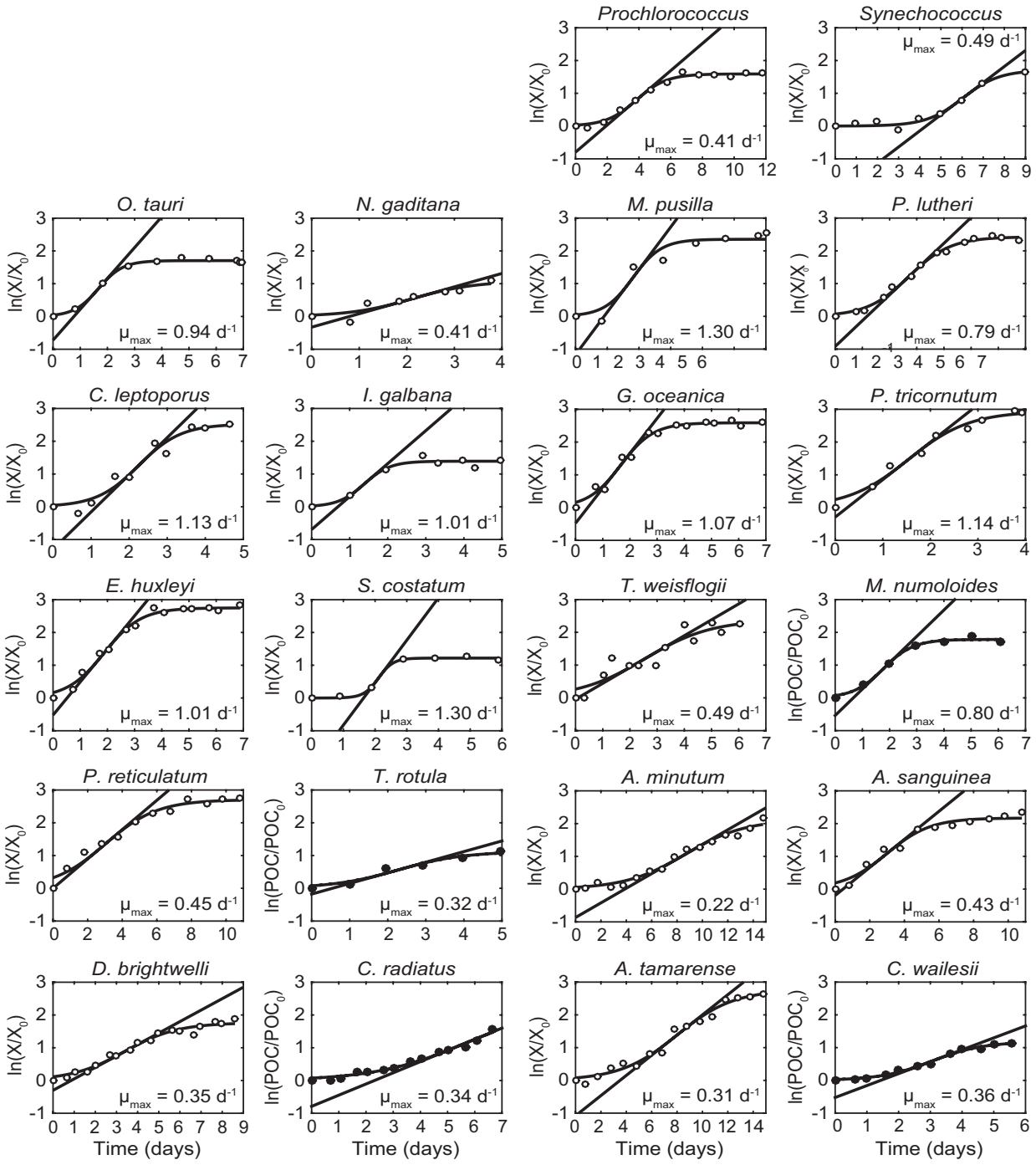

Figure A1: Cellular abundances (X) during the batch culture experiments, normalized to the initial cell abundance in each experiment (X_0). Panels are arranged in order of increasing cell size. Curved lines represent the best fit of equation (A3) to the log-transformed data. Straight lines indicate the tangent to the curve at its inflection point. The gradient of this tangent defines μ_{max}. Filled circles denote species with unreliable cell abundance data. For these species, cell abundance data were substituted with particulate organic carbon data.

 DOI: 10.1086/689992

Appendix B from B. A. Ward et al., "The Size Dependence of Phytoplankton Growth Rates: A Trade-Off between Nutrient Uptake and Metabolism" (Am. Nat., vol. 189, no. 2, p. 000)

Sensitivity to Model Formulation and Possible Biases in the Data

In the main text, we ignored the potential for nutrient uptake to be downregulated as the nutrient quota approaches its maximum capacity. Here we account for this by assuming that the maximum possible rate of nutrient uptake (ρ_{max}) is downregulated as the cell quota (Q) approaches its maximum value (Q_{max}):

$$\rho = \rho_{max}\frac{Q_{max} - Q}{\Delta Q}. \tag{B1}$$

Here ΔQ is defined as $Q_{max} - Q_{min}$ and represents the cellular capacity for nutrient storage above the basal nutrient requirement (Q_{min}). Verdy et al. (2009) showed that when uptake regulation is considered in this way, the maximum per capita growth rate is given by

$$\mu_{max} = \frac{\mu_\infty \rho_{max}}{\mu_\infty Q_{min} + \rho_{max}(Q_{max}/\Delta Q)}. \tag{B2}$$

When we consider this function in two limits, as in equations (4) and (5), we find that equation (4) remains unchanged. If the maximum potential rate of nutrient uptake is assumed to be much slower than the maximum potential rate of cellular metabolism, the maximum growth rate is set by the maximum rate of nutrient uptake relative to the cell's basal nutrient requirement:

$$\mu_{max} \approx \frac{\rho_{max}}{Q_{min}} \text{ if } \rho_{max}\frac{Q_{max}}{\Delta Q} \ll \mu_\infty Q_{min}. \tag{B3}$$

In the alternative limit, if the maximum potential nutrient uptake rate is much faster than the maximum potential rate of cellular metabolism, equation (B2) can be approximated by

$$\mu_{max} \approx \mu_\infty\left(1 - \frac{Q_{min}}{Q_{max}}\right) \text{ if } \rho_{max}\frac{Q_{max}}{\Delta Q} \gg \mu_\infty Q_{min}. \tag{B4}$$

In this limit, the maximum growth rate is now limited by the maximum internal metabolic rate at its maximum quota rather than at infinite quota. Note, however, that if Q_{max} is assumed to be very large relative to Q_{min}, then this second limit can be reasonably approximated by $\mu_{max} \approx \mu_\infty$ (Verdy et al. 2009), as in the main text.

We repeated the model analysis with the maximum quota included as a constraint on nutrient uptake. Observational estimates of Q_{max} were determined for each species as the largest cellular quota recorded in the batch culture experiments of Marañón et al. (2013). Power-law coefficients for Q_{max} were then estimated as for the other three model parameters used in the main text. The four model parameters were then adjusted within uncertainty estimates to maximize the fit of equation (B2) to observed values of μ_{max}.

The results presented in figure B1*A* show that the predicted size dependence of μ_{max} was barely affected by this increase in complexity. This is not to say, however, that Q_{max} is not an important parameter in other aspects of the model behavior, such as the size of the nutrient quota when the nutrient uptake rate (ρ) is much greater than the rate of biomass synthesis (μQ).

We noted in the discussion that the adjusted slopes for ρ_{max} and Q_{min} were at the extremes of the range of values permitted in the optimization process. We attributed this issue to the likely overestimation of Q_{min} among larger cells. To evaluate the credibility of this argument, we repeated the analysis excluding Q_{min} data for cells larger than 6 μm from the analysis. We found that the initial fit of equation (3) had a much steeper slope in the sub 6 μm size range, while the adjusted fit was virtually unchanged (fig. B1*B*). We also found that the adjusted parameter values with the Q_{min} data excluded were within ~1% of their initial values and well within their prior confidence limits (table B1).

Table B1: Initial and adjusted power-law coefficients for each parameter when Q_{min} data for cells larger than 6 μm were excluded from the analysis

		Initial estimates		95% confidence limits		Adjusted estimates	
Parameter aV^b	Units	a	b	a	b	a	b
ρ_{max}	pg N cell^{-1} day^{-1}	.023	.98	.013–.042	.89–1.10	.030	.99
Q_{min}	pg N cell^{-1}	.048	.68	.030–.079	.47–.89	.041	.67
μ_∞	day^{-1}	6.40	−.27	3.6–12.0	−.35 to −.18	4.7	−.26

Note: In this case, all the adjusted power-law coefficients lie well within the prior uncertainty range.

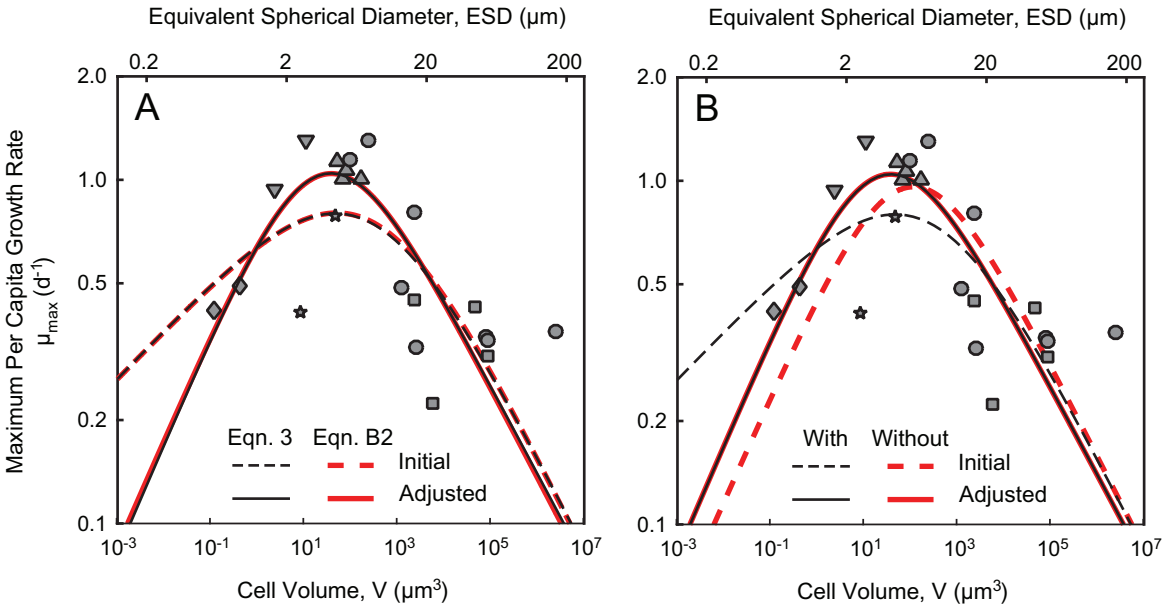

Figure B1: *A*, Comparison of the initial and adjusted fits of the model when also accounting for the maximum nutrient quota. Black lines show the initial and adjusted fits of equation (3). Red lines show the initial and adjusted fits of equation (B2). *B*, Comparison of the initial and adjusted fits of the model with and without Q_{min} data for cells larger than 6 μm equivalent spherical diameter (ESD). Black lines show the initial and adjusted fits of figure 3 with all data included. Red lines show the same fits with the Q_{min} data for larger cells excluded. Diamond, cyanobacteria; down-pointing triangle, chlorophyte; star, other; up-pointing triangle, coccolithophore; circle, diatom; square, dinoflagellate.